

Dynamical Fermions with Fat Links

Francesco Knechtli [†] and Anna Hasenfratz [‡]

Physics Department, University of Colorado, Boulder, CO 80309 USA

We present and test a new method for simulating dynamical fermions with fat links. Our construction is based on the introduction of auxiliary but dynamical gauge fields and works with any fermionic action and can be combined with any fermionic updating. In our simulation we use an over-relaxation step which makes it effective. For four flavors of staggered fermions first results indicate that flavor symmetry at a lattice spacing $a \approx 0.2$ fm is restored to a few percent. With the standard action this amount of flavor symmetry restoration is achieved at $a \approx 0.07$ fm. We estimate that the overall computational cost is reduced by at least a factor 10.

PACS number: 11.15.Ha, 12.38.Gc, 12.38.Aw

December 2000

[†] e-mail: knechtli@pizero.colorado.edu

[‡] e-mail: anna@eotvos.colorado.edu

I. INTRODUCTION

Improved actions reduce lattice artifacts and thus allow simulations at coarser lattice spacing, larger lattice quark masses and smaller lattice volumes. The use of improved actions in large scale numerical simulations has been increasing steadily. For dynamical simulations a factor of two improvement in lattice spacing can easily translate to a gain of 100 in computational cost, which usually more than compensates for the reduction in efficiency of the algorithm. Systematic improvement programs remove lattice artifacts perturbatively [1, 2, 3, 4] or non-perturbatively [5, 6, 7, 8] by adding irrelevant operators to the action. The use of fat or smeared links is part of many of these improvement programs [9, 10]. Smearing the links of a lattice action does not change the long-distance properties of the system but by smoothing out short scale lattice vacuum fluctuations, it reduces lattice artifacts. Fat link actions by themselves show improved scaling properties, especially in quantities most sensitive to short distance fluctuations.

For Wilson-type clover fermions, chiral properties show significant improvement in fat link quenched simulations [11]. Fattening removes many small dislocations and that reduces the spread of the real eigenmodes of the Dirac operator and the occurrence of exceptional configurations. The perturbation theory for fat-link Wilson-type fermions has been worked out in [12], showing that the additive mass renormalization is small, the renormalization factors are very close to one and the tree-level clover coefficient $c_{\text{sw}} = 1.0$ is expected to be close to the non-perturbative value.

Fat links have also been successfully used in overlap actions [13]. The improved chiral properties of fat link actions result in significantly faster convergence in evaluating Neuberger's formula.

The use of fat links with staggered fermions improves flavor symmetry. In the staggered fermion formulation the four components of a Dirac spinor occupy different lattice sites and connect to different gauge fields, leading to flavor symmetry breaking. The flavor symmetry breaking is especially evident for the pions: only one of the pseudoscalar mesons is a true Goldstone particle, the others are massive even at vanishing quark mass. Since flavor symmetry breaking is basically due to the fluctuations of the gauge fields within a hypercube and is particularly sensitive to dislocations, local smearing of the gauge links is very effective in reducing flavor symmetry breaking. Several quenched simulations verified this conjecture [14, 15, 16]. Dynamical simulations with one level of smearing [17, 18] found similar improvement. Perturbative studies of flavor symmetry breaking also support the use of fat links [19].

Dynamical simulation of fermion actions with fat links can be very complicated. Even in the simplest case where the fat link is constructed as a sum of several paths connecting the fermions, the fermionic force term will have many more terms than with thin link action. If the fat link is projected back to $SU(3)$ and the fattening procedure is iterated (as proved to be most effective in quenched simulations), direct calculation of the fermion force term becomes nearly impossible.

In this article we present a new method for simulating fat link fermion actions with many levels of projected smearing. The basic idea is to introduce *an auxiliary but dynamical gauge field* for each smearing level. These gauge fields couple to each other by blocking kernels representing one level of smearing. The last of the auxiliary gauge fields couple directly to the fermions just like ordinary thin links, thus avoiding the complicated gauge force computations. Our construction does not consider the systematic improvement of the action, but it can be combined with any thin link fermionic action. Combining systematic improvements of a thin link action with fat link fermions can lead to further systematic improvement.

To motivate our choice of fat link action in Sect. 2 we study flavor symmetry breaking with staggered fermions in the quenched approximation. We consider valence actions with different levels of smearing and we compare the results with the standard thin link action. The quenched simulation suggests that with three levels of projected fat links flavor symmetry improves to a level corresponding to a factor of 2.5 change in lattice spacing.

In Sect. 3 we present our general construction of a fat link fermion action. We suggest combining different updating methods in the numerical simulation. The simplest is to update the original and all but the last auxiliary gauge fields using Metropolis updating. The last level auxiliary gauge field couples to the fermions. Any fermionic updating can be used, we consider molecular dynamics updating here.

Unfortunately this coupled system is very rigid and evolves extremely slowly under local updating. In Sect. 4 we discuss a global over-relaxation step that improves the situation considerably. Over-relaxation updating based on the gauge action is usually not very effective for fermions [20]. The situation here is quite different. Since the fermions couple to a several times smeared smooth gauge field, we find that one can update up to $(0.3 \text{ fm})^4$ part of the lattice and still have a large enough acceptance rate to make the algorithm efficient.

In Sect. 4 we specify the action for four flavors of staggered fermions and discuss the over-relaxation update in detail. One iteration of our algorithm is composed of 100 over-relaxation, one Metropolis and one molecular dynamics steps. This combined updating is about 15-20 times slower than a molecular dynamics thin link updating and has about the same autocorrelation times. Considering that we gain well over a factor of 100 from the improved scaling properties, this cost is acceptable. Our first results with this algorithm confirms the quenched results for flavor symmetry breaking. We find that flavor symmetry violations are reduced to a few percent at a lattice spacing $a \approx 0.20 \text{ fm}$.

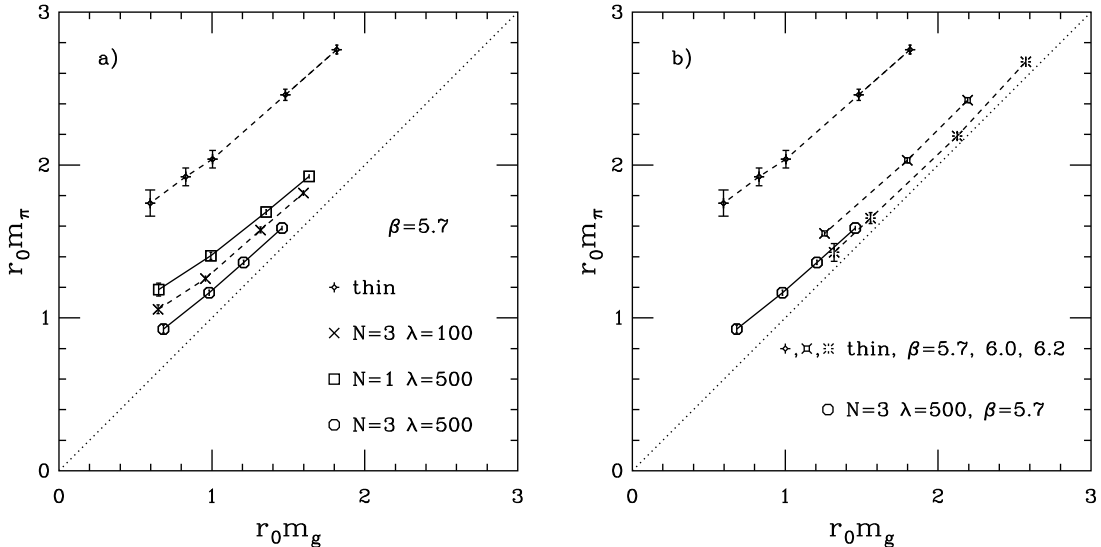


FIG. 1: The mass m_π of the lightest non-Goldstone pion as the function of the mass m_g of the Goldstone pion in the quenched approximation. Fig. 1a) shows results for $\beta = 5.7$ using both a thin link and different fat link valence actions. In Fig. 1b) results obtained with our best fat link action on $\beta = 5.7$ background are compared with thin link action results on $\beta = 5.7$, $\beta = 6.0$ and $\beta = 6.2$ background configurations. The lattice spacing changes by a factor of 2.5 between $\beta = 5.7$ and $\beta = 6.2$.

In Sect. 5 we summarize our results and discuss the future directions.

II. FAT LINK ACTIONS AND QUENCHED SPECTROSCOPY

In this section we investigate the spectrum of fat link staggered actions in the quenched approximation. Previous extensive studies [16] have demonstrated the improvement in the restoration of flavor symmetry due to the smearing of the gauge links. Our goal here is to motivate the parameters of our dynamical fat link action.

We fatten the gauge links using APE smearing [21]: the smeared or fat link Q is constructed from the thin link U as

$$Q_{i,\mu} = (1 - \alpha)U_{i,\mu} + \frac{\alpha}{6}\Sigma_{i,\mu}(U), \quad (1)$$

where $\Sigma_{i,\mu}(U)$ is the sum over the six staples around the link $U_{i,\mu}$. We use the index i to label the lattice sites and the index μ to label the four space-time directions. The smearing procedure eq. (1) can be iterated if the fat link Q is projected to $SU(3)$

$$W_{i,\mu} = \text{Proj}_{SU(3)}\{Q_{i,\mu}\}. \quad (2)$$

The n -th level fat link is given by

$$Q_{i,\mu}^{(n)} = (1 - \alpha)W_{i,\mu}^{(n-1)} + \frac{\alpha}{6}\Sigma_{i,\mu}(W^{(n-1)}), \quad (3)$$

where $\Sigma_{i,\mu}(W^{(n-1)})$ is the sum of staples around $W_{i,\mu}^{(n-1)}$, the $(n-1)$ -th level fat link projected onto $SU(3)$ ($W^{(0)} \equiv U$). In the following we label by N the number of smearing iterations or levels. Perturbative arguments [12] show that for values of the smearing parameter $0 \leq \alpha \leq 0.75$ the smearing orders the gauge configuration suppressing small scale fluctuations. If $\alpha > 0.75$ the smearing eventually disorders. In the following we choose, somewhat arbitrarily, $\alpha = 0.70$.

We consider two different $SU(3)$ projections : a *deterministic* projection $W_{\max,i,\mu}$ defined by

$$\text{ReTr}(W_{\max,i,\mu} Q_{i,\mu}^\dagger) = \max_{W \in SU(3)} \text{ReTr}(W Q_{i,\mu}^\dagger) \quad (4)$$

and a *probabilistic* projection $W_{i,\mu}^\lambda$, where $W_{i,\mu}^\lambda$ is chosen according to the probability distribution

$$P(W) \propto \exp\left[\frac{\lambda}{3}\text{ReTr}(W Q_{i,\mu}^\dagger)\right] \quad (5)$$

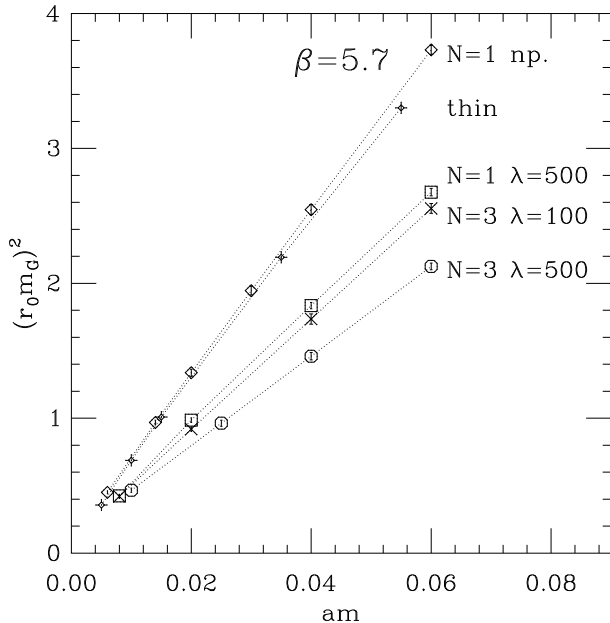


FIG. 2: The mass renormalization in the quenched approximation at $\beta = 5.7$ for the thin link and different fat link valence actions. In addition to the actions used in Fig. 1, we show the results for $N = 1$ level of non-projected (np.) APE smearing.

with projection parameter λ . For $\lambda = \infty$, eq. (5) is equivalent to eq. (4).

To illustrate the effect of fat links on flavor symmetry restoration we calculated the pion spectrum on a set of $8^3 \times 24$, $\beta = 5.7$ ($a = 0.17$ fm) quenched lattices. In Fig. 1a) we plot the masses of the (would-be) Goldstone pion π_g and the lightest non-Goldstone pion, π_{i5} , corresponding to the representation $\gamma_5 \otimes \gamma_i \gamma_5$. We label the representation of the states following [22, 23] by $\Gamma_S \otimes \Gamma_F$, where Γ_S labels the spin and Γ_F labels the SU(4) flavor. The pion masses are expressed in units of the Sommer scale r_0 ($r_0 = 2.87a$ at $\beta = 5.7$) [24]. In addition to the thin link we consider three fat link valence actions: $N = 1$ and $N = 3$ levels of smearing with projection parameter $\lambda = 500$ and $N = 3$ levels of smearing with projection parameter $\lambda = 100$, all with $\alpha = 0.7$. We observe considerable improvement from $N = 1$ to $N = 3$. Also, $\lambda = 100$ for the projection parameter is clearly not as effective as $\lambda = 500$. Increasing the number of blocking levels N or the projection parameter λ further does not improve the situation substantially but increases the computational effort considerably. In the rest of this paper we will consider the fat link action corresponding to $N=3$ levels of blocking with projection parameter $\lambda = 500$ and APE parameter $\alpha = 0.7$. While these parameters are not unique, they seem to be close to optimal.

To get a feel for the amount of improvement one can achieve with this fat link actions, in Fig. 1b) we compare the $N = 3$, $\lambda = 500$ action with thin link data at $\beta = 5.7, 6.0$ and 6.2 . The data for the last two β values are from ref. [23] and correspond to lattice spacings $a = 0.095$ fm and 0.069 fm and Sommer parameters $r_0 = 5.26a$ and $7.25a$, respectively [25]. The $N = 3$, $\lambda = 500$ smearing reduces flavor symmetry violations on the $\beta = 5.7$ configurations to the level obtained at $\beta = 6.2$ with thin link action, a factor of 2.5 improvement in lattice spacing. The computational cost of full QCD grows at least as $1/a^6$ [3] and for certain quantities even as $1/a^{10}$ [26]. A factor 2.5 in the lattice spacing means a factor $200 - 10^4$ in the computational costs.

Finally, in Fig. 2 we plot the square of the Goldstone-pion mass as a function of the bare quark mass. All measurements are on the $\beta = 5.7$ gauge configurations using thin link and different fat link actions. In addition to the actions considered in Fig. 1, we show the results for $N = 1$ level of non-projected APE smearing. Fat link perturbation theory predicts that the mass renormalization constant becomes perturbative as N increases. We see that the mass renormalization after one level of non-projected smearing is almost the same as without smearing. Increasing the smearing level and the value of λ indeed reduces the multiplicative mass renormalization factor.

III. DYNAMICAL FERMIONS WITH FAT LINKS

The quenched results show that smearing the gauge links considerably improves the flavor symmetry of staggered fermions. There is evidence that these results carry over to dynamical simulations [17] where one level of smearing is implemented. Because of the gauge force computations in the molecular dynamics equations of motion, it is very complicated to simulate fermions with many levels of smearing, even impossible if projection of the gauge links onto

$SU(3)$ is made after each smearing step.

Our method to overcome this difficulty is to introduce a set of *auxiliary but dynamical gauge fields* which couple to each other in the action by blocking kernels representing one level of smearing. The last level auxiliary gauge field couples directly to the fermions in the same way the usual thin links do. The problem of the computations of the gauge force is transferred to the gauge sector where it can be solved. This construction can be used for any fermion action which can be simulated with “thin” links.

Let us start considering fermions coupled to fat links constructed with one level of smearing from the thin links $U_{i,\mu}$. We introduce a dynamical auxiliary gauge field V and we define the action

$$S = -\frac{\beta}{3} \sum_p \text{ReTr}(U_p) - \frac{\lambda}{3} \sum_{i,\mu} \text{ReTr}(V_{i,\mu} W_{\max,i,\mu}^\dagger(U)) - \text{tr} \ln[M^\dagger(V)M(V)]. \quad (6)$$

Here p labels the plaquettes U_p , $W_{\max}(U)$ is the $SU(3)$ projection eq. (4) of the fat link given in eq. (1) and $M(V)$ is the fermion matrix. The blocking parameter λ constrains the auxiliary gauge links $V_{i,\mu}$ to be close to the projected fat links $W_{\max,i,\mu}(U)$. Fluctuations of the field V are proportional to $1/\lambda$. This is a dynamical realization of the projection eq. (5). In eq. (6), Tr means the trace over $SU(3)$ color whereas tr means the overall trace over space-time indices i , directions μ , spin and color.

For many levels of smearing, we introduce a set of dynamical auxiliary gauge fields $W^{(1)}, W^{(2)}, \dots, W^{(N)} \equiv V$, one for each level of smearing. The action eq. (6) is generalized to

$$\begin{aligned} S = & -\frac{\beta}{3} \sum_p \text{ReTr}(U_p) - \frac{\lambda}{3} \sum_{i,\mu} \text{ReTr}(W_{i,\mu}^{(1)} W_{\max,i,\mu}^\dagger(U)) \\ & - \frac{\lambda}{3} \sum_{i,\mu} \text{ReTr}(W_{i,\mu}^{(2)} W_{\max,i,\mu}^\dagger(W^{(1)})) \dots - \frac{\lambda}{3} \sum_{i,\mu} \text{ReTr}(V_{i,\mu} W_{\max,i,\mu}^\dagger(W^{(N-1)})) \\ & - \text{tr} \ln[M^\dagger(V)M(V)]. \end{aligned} \quad (7)$$

This action is in the same universality class as the original thin link action. If the blocking parameter is $\lambda = \infty$, the auxiliary gauge fields can be integrated out and the resulting action is a plaquette gauge action while the fermions couple to deterministically projected fat links. If $\lambda \neq \infty$, the integration of the auxiliary gauge fields will introduce additional gauge terms. These new terms depend on the thin link variables in a complicated way, but they are all local terms containing only a finite number of link variables. Thus, these terms do not change the universality class of the action.

The updating of this system can, in principle, be done by a sequence of Metropolis updatings for the fields $U, W^{(1)}, \dots, W^{(N-1)}$ and by the standard updating for the fermion matrix M , with the only difference that now the last auxiliary gauge field V enters the fermion matrix.

The problem of this basic algorithm is that the system with large λ is very rigid and evolves very slowly. To cure this problem, we use a hybrid over-relaxation algorithm [27, 28, 29, 30, 31, 32, 33, 34, 35, 36] with

- ★ Metropolis updating for the gauge fields $U, W^{(1)}, \dots, W^{(N-1)}$,
- ★ standard algorithm for the fermion matrix $M(V)$ and
- ★ *global over-relaxation* for all the gauge fields $U, W^{(1)}, \dots, V$

In the next section we discuss how an over-relaxation can be implemented. It plays a key role in reducing the autocorrelation times of the Metropolis update. Note that the over-relaxation update is effective only because the fermions couple to the smooth fat links.

IV. OVER-RELAXATION WITH FAT LINKS

Our over-relaxation update is based on the usual over-relaxation reflection step used in pure gauge systems that leaves the gauge action invariant [31, 32]. We reflect the original links just like in the standard over-relaxation algorithm

$$U \rightarrow U' \quad (8)$$

followed by a transformation of the fat links

$$W^{(1)\prime} = W^{(1)} W_{\max}^\dagger(U) W_{\max}(U'), \quad (9)$$

$$W^{(2)\prime} = W^{(2)} W_{\max}^\dagger(W^{(1)}) W_{\max}(W^{(1)\prime}), \quad (10)$$

$$\dots \quad V' = V W_{\max}^\dagger(W^{(N-1)}) W_{\max}(W^{(N-1)\prime}). \quad (11)$$

All links for a given level are reflected and then the next level gauge field is changed. The reflections must be performed in the order given by eq. (8)-eq. (11). This transformation leaves the gauge part of the action invariant, but the fermionic part will change and an accept/reject step must be performed.

For the accept-reject step we have to calculate the action, i.e. we need an explicit form of the determinant to evaluate. For four flavors of staggered and two flavors of Wilson fermions this is trivially realized. In terms of pseudofermion fields Φ the action eq. (7) is

$$S = S_g(U, W^{(1)}, \dots, V) + \Phi^\dagger [M^\dagger(V) M(V)]^{-1} \Phi, \quad (12)$$

where $M(V)$ represents the fermion matrix. The equilibrium probability distribution of the gauge fields $U, W^{(1)}, \dots, V$ is given by

$$P_{\text{eq}}(U, W^{(1)}, \dots, V) \propto e^{-S_g(U, W^{(1)}, \dots, V)} \det(M^\dagger(V) M(V)). \quad (13)$$

Since the pure gauge part of the action is invariant under the over-relaxation move of the system, the acceptance probability is

$$P_{\text{acc}}(V', V) = \min \left\{ 1, \frac{\det(M^\dagger(V') M(V'))}{\det(M^\dagger(V) M(V))} \right\}. \quad (14)$$

P_{acc} depends only on the last level auxiliary gauge links. The goal is to efficiently compute the acceptance probability.

Instead of calculating the determinant in eq. (13) we use a stochastic estimator to approximate P_{acc} [37, 38]

$$P_{\text{acc}}(V', V) = \min \left\{ 1, e^{\xi^\dagger [M^\dagger(V') M(V') - M^\dagger(V) M(V)] \xi} \right\}, \quad (15)$$

where the vector ξ is generated according to the distribution

$$P(\xi) \propto e^{-\xi^\dagger M^\dagger(V') M(V') \xi}. \quad (16)$$

After configuration averaging, this procedure satisfies the detailed balance condition [38].

If the gauge fields V and V' are very different, the acceptance rate from eq. (15) will be small even when the fermionic determinants are actually very close. This is because of the large fluctuations of the stochastic estimator. To improve the acceptance rate, we attempt to remove the most ultraviolet part of the fermionic matrix and include it explicitly as an effective gauge action. The resulting reduced matrix gives a much higher acceptance in eq. (15).

For heavy fermions the fermion determinant gives rise to an effective plaquette term for the gauge field [39]. Even for small quark masses the ultraviolet part of the fermion determinant can be well approximated by an effective loop action involving only small Wilson loops [40, 41]. These observations suggest to remove the plaquette term from the fermion matrix by introducing a reduced matrix M_r as

$$M(V) = M_r(V) A(V) \quad \text{with} \quad (17)$$

$$A(V) = e^{\alpha_4 D^4(V) + \alpha_2 D^2(V)}, \quad (18)$$

where D is the kinetic part of the fermion matrix. In terms of M_r the fermion determinant becomes

$$\det(M^\dagger(V) M(V)) = \det(M_r^\dagger(V) M_r(V)) e^{-S_{\text{eff}}(V)}, \quad (19)$$

$$S_{\text{eff}}(V) = -2\alpha_4 \text{Retr}[D^4(V)] - 2\alpha_2 \text{Retr}[D^2(V)]. \quad (20)$$

The effective action $S_{\text{eff}}(V)$ can be evaluated explicitly. In general it is the sum of a plaquette term coming from $\text{tr}[D^4(V)]$ and a constant from $\text{tr}[D^2(V)]$. The real parameters α_2 and α_4 are free and can be optimized. In a different context, a decomposition of the fermion matrix like eq. (17) has been proposed in [20] motivated by the hopping parameter expansion.

In terms of $S_{\text{eff}}(V)$ and $M_r(V)$ the acceptance probability is

$$P_{\text{acc}}(V', V) = \min \left\{ 1, \frac{e^{-S_{\text{eff}}(V')} \det(M_r^\dagger(V') M_r(V'))}{e^{-S_{\text{eff}}(V)} \det(M_r^\dagger(V) M_r(V))} \right\}, \quad (21)$$

$$= \min \left\{ 1, e^{S_{\text{eff}}(V) - S_{\text{eff}}(V') + \xi^\dagger [M_r^\dagger(V') M_r(V') - M_r^\dagger(V) M_r(V)] \xi} \right\}. \quad (22)$$

where the vector ξ is now generated according to the distribution

$$P(\xi) \propto e^{-\xi^\dagger M_r^\dagger(V') M_r(V') \xi}. \quad (23)$$

In practice, we start by generating a random Gaussian source R according to the probability distribution

$$P(R) \propto e^{-R^\dagger R} \quad (24)$$

from which we form the vectors

$$\Phi' = M^\dagger(V') R, \quad (25)$$

$$X' = [M^\dagger(V') M(V')]^{-1} \Phi'. \quad (26)$$

The vector ξ in eq. (23) is then given by $\xi = A(V') X'$ and we can write the fermionic terms in eq. (22) as

$$\xi^\dagger M_r^\dagger(V') M_r(V') \xi = \Phi'^\dagger X', \quad (27)$$

$$\xi^\dagger M_r^\dagger(V) M_r(V) \xi = X'^\dagger A^\dagger(V') A^\dagger(V)^{-1} M^\dagger(V) M(V) A(V)^{-1} A(V') X'. \quad (28)$$

The acceptance probability strongly depends on the parameters α_2 and α_4 . The optimal value can be found numerically. We will discuss our choice in the next section.

This procedure is not effective if the fermion matrix depends on thin links, because the fluctuations in the stochastic estimator are too large even after the removal of the D^4 and D^2 terms. When the links in the fermion matrix are smeared, these fluctuations are constrained. This is the key feature which makes the over-relaxation effective with fat links.

This over-relaxation algorithm is a legal update of the system. The reversibility of the reflections (primed and unprimed quantities can be exchanged in eq. (8)-eq. (11)) ensures that the detailed balance condition is satisfied. To achieve ergodicity though, one must still perform some updatings with the basic algorithm.

V. PERFORMANCE OF THE ALGORITHM

For testing our fat link action we decided to simulate $N_f = 4$ flavors of staggered fermions. The fermion matrix is given by

$$M(V)_{i,j} = 2m\delta_{i,j} + \sum_{\mu} \eta_{i,\mu} (V_{i,\mu} \delta_{i,j-\hat{\mu}} - V_{i-\hat{\mu},\mu}^\dagger \delta_{i,j+\hat{\mu}}), \quad (29)$$

where $\eta_{i,\mu}$ are the staggered phases. We impose anti-periodic boundary conditions in the time direction. The pseudofermion field Φ and the matrix $M^\dagger(V) M(V)$ are restricted to the even sites of the lattice [42]. The matrix D used in eq. (18) is given by

$$D_{i,j} = \sum_{\mu} \eta_{i,\mu} (V_{i,\mu} \delta_{i,j-\hat{\mu}} - V_{i-\hat{\mu},\mu}^\dagger \delta_{i,j+\hat{\mu}}). \quad (30)$$

The traces in $S_{\text{eff}}(V)$ in eq. (20) are computed by summing over the even sites only and give

$$\text{tr}[D^4(V)] = 24\Omega [3 - \frac{1}{6\Omega} \sum_{\mathbf{p}} \text{ReTr}(V_{\mathbf{p}})] + 108\Omega - 4\delta_{N_t,4} \sum_{i,t=0} \text{ReTr}(P_i), \quad (31)$$

$$\text{tr}[D^2(V)] = -12\Omega. \quad (32)$$

Ω denotes the total number of lattice points and we assume that there are more than 4 sites in each space-like direction. For $N_t = 4$ sites in the time-like direction there is an extra contribution to $\text{tr}[D^4(V)]$ coming from the Polyakov lines

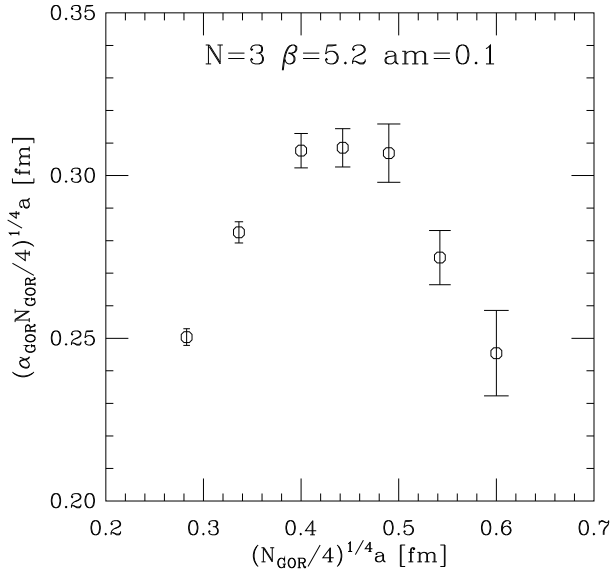


FIG. 3: The effective physical volume where the U links change in one global over-relaxation (GOR) updating step as function of the physical volume “touched”. The results are obtained on $8^3 \times 24$ lattices.

P_i starting at location $i, t = 0$. The minus sign of the Polyakov line in eq. (31) is due to the anti-periodic boundary conditions in time direction.

As we described in Sect. 2 we choose the number of auxiliary gauge fields and the smearing parameters to be

$$N = 3, \alpha = 0.7, \lambda = 500. \quad (33)$$

The global over-relaxation (GOR) described in Sect. 4 is essential here as it considerably reduces the autocorrelations of the otherwise very rigid system. The GOR leaves the pure gauge action of our system invariant but is subjected to an accept/reject step which accounts for the ratio of fermion determinants, see eq. (22). Since the fermions couple directly to the last level dynamical fat links, the acceptance rate α_{GOR} is large enough to make the algorithm effective.

The parameters α_2 and α_4 entering eq. (18) are chosen to maximize the acceptance rate α_{GOR} . We use

$$\alpha_2 = -0.18, \alpha_4 = -0.006. \quad (34)$$

Setting $\alpha_2 = \alpha_4 = 0$, i.e. computing the ratio of fermion determinants without decomposing the fermion matrix according to eq. (17) and eq. (18) gives a value for α_{GOR} which is a factor 10 smaller than what we achieve with our choice. Moreover, keeping $\alpha_4 = 0$ and varying only α_2 gives significantly lower α_{GOR} . The choice of eq. (34) is not unique, we identified in the $\alpha_2 - \alpha_4$ parameter space a band-like region in which α_{GOR} reaches its maximal value.

Even with our improved GOR it is not possible to change simultaneously all the U links, the effectiveness of the algorithm would be very low. Instead we choose a random block of U links containing $(N_{\text{GOR}}/4)$ sites and reflect only the links within this block. These changes propagate more and more through the lattice as we consider the cascade of reflections eq. (8)-eq. (11), as 19 fat links have to be changed by changing one link. In Fig. 3 we plot the volume of the lattice in which the U links are effectively updated (actually the fourth root of it), i.e. $(\alpha_{\text{GOR}} N_{\text{GOR}}/4)^{1/4}a$ as function of the physical volume of the “touched” U links $(N_{\text{GOR}}/4)^{1/4}a$. These results are obtained on $8^3 \times 24$, $\beta = 5.2$ and $am = 0.1$ lattices. The lattice spacing from the string tension can be estimated as $a \approx 0.2$ fm and the correlation length as $r_0 m_g \approx 1.7$. We see in Fig. 3 that there is a maximal physical volume

$$V_{\text{GOR}} \approx (0.3 \text{ fm})^4 \quad (35)$$

which can be updated with a reasonable acceptance rate. The actual value of α_{GOR} depends on the number of “touched” links N_{GOR} . The broad maximum in Fig. 3 corresponds to $\alpha_{\text{GOR}} = 35\%$ ($N_{\text{GOR}} = 64$), $\alpha_{\text{GOR}} = 24\%$ ($N_{\text{GOR}} = 96$) and $\alpha_{\text{GOR}} = 15\%$ ($N_{\text{GOR}} = 144$) on the above lattices.

We observed that the value eq. (35) scales with the lattice spacing. On lattices with smaller lattice spacing more links can be updated at the same time, i.e. the physical volume of the updated region remains fixed. On larger physical volumes, on the other hand, one would have to increase the number of GOR steps to achieve the same efficiency. In our finite-temperature runs on $8^3 \times 4$ lattices [43] we observed that the effectiveness of the algorithm increases in the deconfined phase.

links	100 × GOR	1 × MET	1 × HMC	total	CG iterations
“thin”	-	-	1	1	133
fat	11.0	3.5	0.5	15.0	61

TABLE I: Timings for simulation of ordinary thin link HMC algorithm compared to simulation of our algorithm with $N = 3$ auxiliary gauge fields. The dynamical lattices are $8^3 \times 24$ and the lattice spacings and physical quark masses of the two simulations are approximately matched. The time unit is one updating step (consisting of one HMC trajectory) of the ordinary thin link algorithm. The last two columns give the total time costs and the average number of conjugate gradient (CG) iterations needed for inversion of $M^\dagger M$.

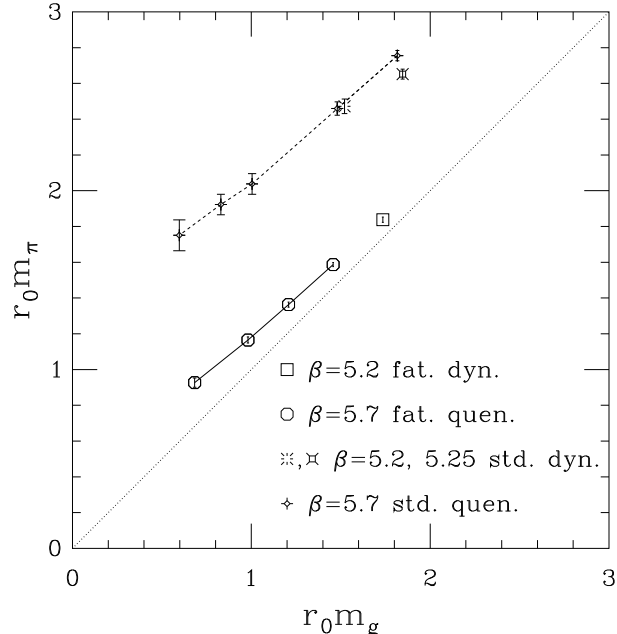


FIG. 4: Flavor symmetry violation for the dynamical runs with our fat link action (fat. dyn.) and with the standard thin link staggered action (std. dyn.). The lattice spacings and the correlation lengths are approximately matched. For comparison we plot the quenched results from Fig. 1 obtained with the corresponding valence actions (fat. quen. and std. quen.).

In simulating the $8^3 \times 24 \approx 20 \text{ fm}^4$ lattices, we found it effective to follow each Metropolis and HMC by 100 GOR updating steps, each reflecting about $(0.3 \text{ fm})^4$ section of the thin link lattices. For timing our algorithm we consider the computer time necessary for 100 GOR steps, one Metropolis (MET) step for each gauge field $U, W^{(1)}, W^{(2)}$ and one HMC trajectory for the V field with step size $\Delta t = 0.015$ and $N_{\text{traj}} = 30$ steps. We compare this to the time of one HMC trajectory with step size $\Delta t = 0.015$ and $N_{\text{traj}} = 30$ steps for the thin link action [44, 45] with parameters $\beta = 5.25$ and $am = 0.06$. With these parameters the lattice spacings and the physical quark masses of the two actions are approximately matched. To compare the times for one updating iteration is fair because the autocorrelations for simple observables like the plaquette or the chiral condensate $\psi\psi$ are observed to be the same for the two algorithms in these time units.

In Table I we show the results of the timing comparison. We use one iteration of ordinary thin link HMC as time unit. One iteration of our algorithm costs a factor 15 more but, as pointed out in Sect. 2, we can effectively gain a factor $10^2 - 10^4$ in computer time due to improved scaling. With fat links, there is also a considerable reduction (a factor 2) in the number of conjugate gradient (CG) iterations needed for the inversion of $M^\dagger M$, as shown in the last column of Table I.

Finally we consider flavor symmetry restoration on the dynamical fat link lattices. Fig. 4 shows the first results obtained with our fat link action on $8^3 \times 24$ lattices with parameters $\beta = 5.2, am = 0.1$ (square). This point agrees very well with the quenched results (octagons) taken from Fig. 1, i.e. flavor symmetry violation is reduced to a few percent. To show the improvement due to the smearing of the gauge links, we also ran the standard thin link staggered action with two sets of parameters, $\beta = 5.25, am = 0.06$ (fancy square) and $\beta = 5.2, am = 0.06$ (burst). The lattice spacings from the string tension are approximately $a \approx 0.18 \text{ fm}$ and $a \approx 0.22 \text{ fm}$, and the correlation lengths are $r_0 m_g \approx 1.8$ and $r_0 m_g \approx 1.5$, respectively. The flavor symmetry violations on the thin link dynamical lattices agree with the quenched predictions (fancy diamonds). Our fat link dynamical action has only about 6% flavor symmetry

violation compared to 60% of thin link actions at comparable lattice spacings.

VI. CONCLUSIONS

We presented a new method for simulating dynamical fermions with fat links constructed through many levels of projected smearing. For each level of smearing we introduce an auxiliary but dynamical gauge field and these gauge fields are connected to each other by blocking kernels representing one level of smearing. Since the last of the auxiliary fields couple in the standard way to the fermions, our construction can be used with any known fermionic update. We discussed the simulation of our system which includes an over-relaxation updating. The fat links entering the fermion matrix make the over-relaxation effective and this is the key feature of our algorithm.

At this time our algorithm is running on scalar machines and the over-relaxation step is worked out for four flavors of staggered fermions. The results for flavor symmetry restoration confirm the quenched results, that is, a factor 2.5 in the lattice spacing can be gained. Taking into account that our algorithm is about 15-20 times slower than the standard one, this gives an overall gain of at least a factor 10 in computational costs.

We have used this algorithm to study the finite temperature phase transition of four flavors of staggered fermions at $N_t = 4$ [43]. We observe a qualitative difference compared to thin link simulations. The strongly first order phase transition is washed away, we observe a very broad crossover instead. We believe this difference is due to the improved flavor symmetry. In our simulations we have 15 relatively light pions compared to the single Goldstone particle of thin link simulations.

We are parallelizing the code for large scale simulations [46]. This requires a 32-checkerboard structure but it is not more complicated than parallelizing a Symanzik improved gauge action. The over-relaxation generalizes easily for two flavors of Wilson fermions. To generalize it for two flavors of staggered fermions we need an explicit realization of the action. That can be done by approximating the square root of the fermionic determinant with a polynomial form [47, 48]. Our preliminary study shows that it can be done efficiently.

Acknowledgment. We are indebted to the MILC Collaboration for the use of their code for standard staggered fermions. We thank Thomas DeGrand for many useful discussions. This work was supported by the U.S. Department of Energy.

[1] K. Symanzik, Nucl. Phys. B226 (1983) 187.
[2] K. Symanzik, Nucl. Phys. B226 (1983) 205.
[3] G.P. Lepage, Nucl. Phys. Proc. Suppl. 47 (1996) 3, hep-lat/9510049.
[4] M. Alford, T.R. Klassen and G.P. Lepage, Phys. Rev. D58 (1998) 034503, hep-lat/9712005.
[5] P. Hasenfratz and F. Niedermayer, Nucl. Phys. B414 (1994) 785, hep-lat/9308004.
[6] T. DeGrand, A. Hasenfratz, P. Hasenfratz and F. Niedermayer, Nucl. Phys. B454 (1995) 587, hep-lat/9506030.
[7] T. DeGrand, A. Hasenfratz, P. Hasenfratz and F. Niedermayer, Nucl. Phys. B454 (1995) 615, hep-lat/9506031.
[8] W. Bietenholz and U.J. Wiese, Nucl. Phys. B464 (1996) 319, hep-lat/9510026.
[9] MILC, T. DeGrand, Phys. Rev. D58 (1998) 094503, hep-lat/9802012.
[10] F. Niedermayer, P. Rufenacht and U. Wenger, (2000), hep-lat/0007007.
[11] T. DeGrand, A. Hasenfratz and T. Kovacs, Nucl. Phys. B547 (1999) 259.
[12] C. Bernard and T. DeGrand, Nucl. Phys. Proc. Suppl. 83 (2000) 845, hep-lat/9909083.
[13] MILC, T. DeGrand, (2000), hep-lat/0007046.
[14] T. Blum et al., Phys. Rev. D55 (1997) 1133, hep-lat/9609036.
[15] J.F. Lagae and D.K. Sinclair, Phys. Rev. D59 (1999) 014511, hep-lat/9806014.
[16] MILC, K. Orginos, D. Toussaint and R.L. Sugar, Phys. Rev. D60 (1999) 054503, hep-lat/9903032.
[17] MILC, K. Orginos and D. Toussaint, Phys. Rev. D59 (1999) 014501, hep-lat/9805009.
[18] F. Karsch, E. Laermann and A. Peikert, Phys. Lett. B478 (2000) 447, hep-lat/0002003.
[19] G.P. Lepage, Phys. Rev. D59 (1999) 074502, hep-lat/9809157.
[20] M. Hasenbusch, Phys. Rev. D59 (1999) 054505, hep-lat/9807031.
[21] APE, M. Albanese et al., Phys. Lett. 192B (1987) 163.
[22] H. Kluberg-Stern, A. Morel, O. Napoly and B. Petersson, Nucl. Phys. B220 (1983) 447.
[23] R. Gupta, G. Guralnik, G.W. Kilcup and S.R. Sharpe, Phys. Rev. D43 (1991) 2003.
[24] R. Sommer, Nucl. Phys. B411 (1994) 839, hep-lat/9310022.
[25] ALPHA, M. Guagnelli, R. Sommer and H. Wittig, Nucl. Phys. B535 (1998) 389, hep-lat/9806005.
[26] F. Niedermayer, Nucl. Phys. Proc. Suppl. 53 (1997) 56, hep-lat/9608097.
[27] R. Gupta et al., Phys. Rev. Lett. 61 (1988) 1996.
[28] J. Apostolakis, C.F. Baillie and G.C. Fox, Phys. Rev. D43 (1991) 2687.
[29] M. Hasenbusch and S. Meyer, Phys. Rev. D45 (1992) 4376.

- [30] U. Wolff, Phys. Lett. B284 (1992) 94, hep-lat/9205001.
- [31] M. Creutz, Phys. Rev. D36 (1987) 515.
- [32] F.R. Brown and T.J. Woch, Phys. Rev. Lett. 58 (1987) 2394.
- [33] K.M. Decker and P. de Forcrand, Nucl. Phys. Proc. Suppl. 17 (1990) 567.
- [34] R. Gupta, G.W. Kilcup, A. Patel, S.R. Sharpe and P. de Forcrand, Mod. Phys. Lett. A3 (1988) 1367.
- [35] UKQCD, S.P. Booth et al., Phys. Lett. B275 (1992) 424.
- [36] U. Wolff, Phys. Lett. B288 (1992) 166.
- [37] M. Grady, Phys. Rev. D32 (1985) 1496.
- [38] M. Creutz, *Algorithms for simulating fermions*, Advanced Series on Directions in High Energy Physics-Vol. 11 Quantum fields on the computer (ed. M. Creutz) .
- [39] A. Hasenfratz and T.A. DeGrand, Phys. Rev. D49 (1994) 466, hep-lat/9304001.
- [40] A. Duncan, E. Eichten and H. Thacker, Phys. Rev. D59 (1999) 014505, hep-lat/9806020.
- [41] A. Duncan, E. Eichten, R. Roskies and H. Thacker, Phys. Rev. D60 (1999) 054505, hep-lat/9902015.
- [42] O. Martin and S.W. Otto, Phys. Rev. D31 (1985) 435.
- [43] A. Hasenfratz and F. Knechtli, in preparation .
- [44] S. Gottlieb, W. Liu, D. Toussaint, R.L. Renken and R.L. Sugar, Phys. Rev. D35 (1987) 2531.
- [45] S. Duane, A.D. Kennedy, B.J. Pendleton and D. Roweth, Phys. Lett. B195 (1987) 216.
- [46] T. DeGrand, A. Hasenfratz and F. Knechtli, in preparation .
- [47] T. Takaishi and P. de Forcrand, (2000), hep-lat/0011003.
- [48] I. Montvay, Nucl. Phys. B466 (1996) 259, hep-lat/9510042.